Revista Brasileira de Geografia Física v.18, n.03 (2025) 1721-1723.

ISSN:1984-2295

Revista Brasileira de Geografia Física

Homepage:https://periodicos.ufpe.br/revistas/rbgfe

Comparing the ultraviolet index at sea level and altitude in six Chilean locations

Marcelo de Paula Corrêa[1], Miguel Rivas[2a], Elisa Rojas[2b], Sasha Madronich[3], David Laroze[4], Laura Milena Pérez[5], Juan Crespo Fuentes[6a], Gastón Torres[6b]

[1]Full Professor, Director of the Natural Resources Institute, Universidade Federal de Itajubá, Av. BPS 1303, CEP 37500-903, Itajubá/MG, Brazil, e-mail: mpcorrea@unifei.edu.br, ORCID: 0000-0002-4821-3828; [2]Departamento de Física, Universidad de Tarapacá, Av. 18 de Septiembre n° 2222, 1000000, Arica y Parinacota, Chile, [a]Retired professor, e-mail: mrivas@uta.cl, ORCID: 0009-0005-6388-5648; [b]Retired professor, e-mail: erojas@uta.cl ORCID: 0009-0007-1022-0284; [3]Senior researcher, Atmospheric Chemistry Division, National Centre for Atmospheric Research, 1850 Table Mesa Dr, Boulder, CO 80305, USA, e-mail: sasha@ucar.edu, ORCID: 0000-0003-0983-1313; [4] Diretor, Instituto de Alta Investigación, Universidad de Tarapacá, Casilla 7 D, Arica, Chile.e-mail: dlarozen@academicos.uta.cl. ORCID: 0000-0002-6487-8096; [5]Associate professor, Departamento de Ingeniería Industrial y de Sistemas, Facultad de Ingeniería, Universidad de Tarapacá, Av. 18 de Septiembre n° 2222, 1000000, Arica y Parinacota, Chile, e-mail: lperez@academicos.uta.cl, ORCID: 0000-0002-2915-309X; [6]Subdepartamento de Climatología y Meteorología Aplicada, Dirección Meteorológica de Chile, Av. Portales 3450, Estación Central, 9160000, Santiago, Chile, [a]Meteorologist, e-mail: juan.crespo@dgac.gob.cl, ORCID: 0009-0006-3663-2941, [b] Meteorologist, e-mail: gtorres@meteochile.cl, ORCID: 0009-0006-0783-6064.

Artigo recebido em 31/10/2024 e aceito em 24/01/2025

A B S T R A C T

This study examines the variability of the Ultraviolet Index (UVI) across different altitudes in Chile, analyzing simultaneous UVI measurements from six meteorological stations located at both sea level and high altitudes. The key findings include: UVI increases with altitude: In all regions studied, UVI levels were significantly higher at elevated locations than in coastal areas. For instance, UVI ratios between high and low-altitude sites ranged from 1.14 to 1.39, indicating up to 39% higher UV exposure at greater heights. High UVI values in risk categories: Alarmingly, more than 50% of the UVI measurements surpassed the high-risk threshold in several high-altitude areas. In the Atacama region, over 60% of UVI values exceeded 11, considered highly harmful. Altitude effect on UVI: The altitude effect (AE), calculated as the percentage increase in UVI per 1000 meters, ranged from 5.7% to 11.6%, with higher values in regions with more significant altitude differences. Discrepancies between modeled and measured UVI: The Tropospheric Ultraviolet and Visible (TUV) radiation model overestimated UVI values by 15–27% under clear-sky conditions, highlighting the influence of local factors like cloud cover, aerosols, and surface reflectance on UV exposure.

These results underscore the urgent need for increased awareness of UV risks at high altitudes, particularly for those involved in outdoor activities in these regions. The study advocates for more robust public health initiatives to ensure adequate sun protection in high UV environments.

Comparação do índice ultravioleta ao nível do mar e em altitude em seis localidades chilenas

R E S U M O

Este estudo examina a variabilidade do Índice Ultravioleta (IUV) em diferentes altitudes no Chile, analisando medições simultâneas do IUV de seis estações meteorológicas localizadas ao nível do mar e em altitudes elevadas. As principais descobertas incluem: O IUV aumenta com a altitude: em todas as regiões estudadas, os níveis de IUV foram significativamente maiores em locais elevados do que em áreas costeiras. Por exemplo, as proporções de IUV entre locais de alta e baixa altitude variaram de 1,14 a 1,39, indicando até 39% mais exposição à radiação UV em altitudes maiores. Altos valores de IUV em categorias de risco: de modo preocupante, mais de 50% das medições de IUV ultrapassaram o limite de alto risco nas áreas de alta altitude. Na região do Atacama, mais de 60% dos valores de IUV excederam 11, considerado altamente prejudicial à saúde. Efeito da altitude no IUV: O efeito da altitude (EA), calculado como o aumento percentual no IUV a cada 1000 metros de elevação, variou de 5,7% a 11,6%, com valores mais altos em regiões com diferenças de altitude mais significativas. Discrepâncias entre o UVI modelado e medido: O modelo de radiação ultravioleta e visível troposférica (TUV) superestimou os valores do UVI em 15–27% em condições de céu limpo, destacando a influência de fatores locais como cobertura de nuvens, aerossóis e refletância da superfície na exposição ao UV. Esses resultados ressaltam a necessidade urgente de maior conscientização sobre os riscos de UV em grandes altitudes, principalmente para aqueles envolvidos em atividades ao ar livre nessas regiões. O estudo defende iniciativas de saúde pública mais robustas para garantir proteção solar adequada em ambientes com alto nível de UV.

Introduction

Solar ultraviolet radiation (UVR) is related to the Earth's life. It is a critical component of Earth's energy system, driving numerous photochemical and photobiological processes in the atmosphere and on the surface. Because of its high energy, it is responsible for several photochemical and photobiological processes in the atmosphere and surface. UVR plays a dual role in both sustaining and threatening life. It has been known for a long time that each species of living beings, including different individuals within a species, has a different response to a given UVR dose (Zerefos et al., 2023; Frazão et al, 2024).

In humans, UVR is responsible for several health injuries. UVR is a significant cause of skin damage, including erythema (skin reddening caused by sunburn), premature aging, and skin cancers such as melanoma, basal cell carcinoma, and squamous cell carcinoma. Recent research has shown that UVR-induced DNA damage and oxidative stress are key mechanisms underlying these effects (Zerefos et al., 2023; Frazão et al., 2024). Patra et al. (2023) recently demonstrated that UVR exposure alters the skin microbiome, potentially exacerbating inflammatory responses and increasing cancer risk.

In addition, UVR can also cause eye problems, hair damage, and immune system depletion. Hatsusaka et al. (2021) found that UVR-induced oxidative stress in the lens and cornea contributes to cataract formation, particularly in populations living in high-altitude regions. Ding et al. (2024) highlighted the role of UVR in developing pterygium, emphasizing the need for protective measures in high-exposure areas.

Emerging research by Ceridian et al. (2025) has shown that UVR degrades hair proteins, leading to structural damage, loss of color, and reduced tensile strength. A study by Bloch et al. (2021) corroborates these findings, demonstrating that UVR exposure increases hair porosity and brittleness.

UVR overexposure can suppress local and systemic immune responses, increasing infection susceptibility and reducing vaccine efficacy. Hart and Norval (2021) identified the modulation of cytokines and immune cell activity as key mechanisms. A recent study shows that UVR exposure alters the expression of immune-related genes, further compromising immune function (Liang et al., 2024). For those reasons, knowing UVR availability at a given point on the Earth is essential for public information.

Information on UVR levels for the population is essential for preventing the health damages mentioned above. In this way, the World Health Organization recommends the disclosure of the Ultraviolet Index (UVI) (WHO, 2002). UVI is a unitless scale (Table 1) based on the spectral UVR weighted by the erythemal response spectrum (ISO/CIE, 1999). This weighted irradiance is called erythemal UV irradiance and represents the sensitivity of human skin to different UVR wavelengths. Each UVI unit is equivalent to 25 mWm^{-2} of erythemal irradiance.

Table 1. Solar Ultraviolet Index (UVI) scale, solar risk and reccomended protection according to WHO recommendations

UVI	Solar Risk	Protection
1 – 2	Low	No protection needed
3 – 5	Medium	Necessary protection
6 – 7	High	Essential protection
8 – 10	Very High	Extra protection is required
11+	Extreme	

UVR and UVI availability at the surface depends on temporal (time of day and season), atmospheric (total ozone content, aerosols, and clouds), and geographical (latitude, longitude, and altitude) factors (Corrêa, 2015; WMO, 2022). The stratospheric ozone strongly absorbs UVR, while clouds and particulate matter scatter it. Climate change is altering atmospheric composition, affecting UVR levels. Recent studies evaluated the effects of climate change on these atmospheric constituents and their impacts on UVR availability (Barnes et al., 2019; Corrêa et al., 2019; Yamamoto et al., 2024b). Arias et al. (2022) projected that climate change will exacerbate UVR variability, particularly in high-altitude regions, due to changes in cloud cover and ozone dynamics.

Higher UVR levels are typically observed around solar noon in Earth's tropical and subtropical regions during summertime (Silva et al., 2019; Yamamoto et al., 2024a). Furthermore, in elevated areas of the planet, the UVR also tends to be higher once the rarefaction of the atmosphere reduces the scattering of gases and particles. UVR increases by approximately 10 to 20% per 1,000 meters of elevation depending on surface conditions (Corrêa, 2015; WMO, 2022; Schmalwieser, 2021). Vuilleumier et al. (2020) used satellite data to map UVI variability across different altitudes, highlighting the disproportionate exposure risks in high-altitude regions. In this context, studying the effect of increases in UVR due to the rise in altitude constitutes a significant field of knowledge.

The north of Chile is a desert area with a significant altitude gradient. The distance between the sea-level coastal zone and the highlands, which reach more than 4000 m, is only 150 km. The highlands are part of the Andes Mountains located in a large region between latitudes 12º-24º S and longitudes 65º-71º W. This unique geography, with its steep altitude gradient from sea level to over 4,000 meters, provides an ideal setting for studying UVR variability. As mentioned above, the availability of solar radiation differs strongly between these regions and increases with altitude. This can have important consequences on human health once significant increases in UVR can be perceived when people move from sea level to highland areas.

The rapid increase in UVR with altitude poses significant health risks, particularly for individuals with lighter skin phototypes. Furthermore, people need an adaptation period from a lower to a higher UVR exposure. After all, the incidence of skin cancer has increased in Chile (Alonso et al, 2005). For the predominant phototypes in Chile, skin type III in women, and skin type IV in men (Fitzpatrick, 1988; Zemelman et al, 2001), the adaptation period for skin tanning is at least three days (Cabrera et al., 1985). For this reason, intense and episodic sun exposure for short periods, such as a leisurely weekend in the mountains, can be extremely harmful to skin health. Recent studies have shown that even short-term exposure to high-altitude UVR, such as during weekend trips, can be harmful (Cabrera et al., 1985; Frazão et al., 2024). Unlike other types of cancer, skin cancer is more prevalent in high-altitude populations compared to low-altitude populations, underscoring the need for targeted public health interventions (Gerstein & Samaniego, 2021).

The human skin requires time to adapt to increased UVR exposure through melanin production and thickening of the epidermis. This adaptation period is at least three days for individuals with skin types III and IV (Cabrera et al., 1985). Without proper acclimatization, episodic exposure to high UVR levels can be particularly damaging. Several studies emphasized the importance of public education campaigns to promote gradual acclimatization and protective measures (Kliniec et al., 2023; Marilyn et al., 2024).

Recent technological advancements have improved our ability to monitor and predict UVR levels. Satellite-based instruments and ground-based sensors now provide high-resolution data on UVI variability, enabling more accurate public health recommendations. Studies using data from satellites such as NASA's OMI (Ozone Monitoring Instrument), ESA's Global Ozone Monitoring Experiment - 2 (GOME-2), and ESA's Sentinel-5P TROPOMI (TROPOspheric Monitoring Instrument) have been provided detailed maps UVI distribution, highlighting the influence of altitude, ozone, and aerosols (Parisi et al., 2021; Reshi et al., 2024). In parallel, ground-based networks, such as those established in Chile, have been instrumental in understanding local UVR variability and validating these satellite data. The results of this work could also contribute to validating this type of remote data.

Given this context, the present study evaluated the variability of a large set of UVI measurements carried out in 3 pairs of locations, one close to sea level and the other at high altitude, in different regions of Chile. This paper highlights the strong relationship between altitude and UVR levels due to reduced atmospheric scattering and absorption at higher elevations. This hypothesis aims to quantify the extent of this variability and identify the key atmospheric drivers. We hope this analysis contributes to further studies on UVI variation with altitude.

Methods

Sites of measurements

Simultaneous UVR measurements were performed between 2017 and 2019 in six meteorological stations at different altitudes, as shown in Figure 1.

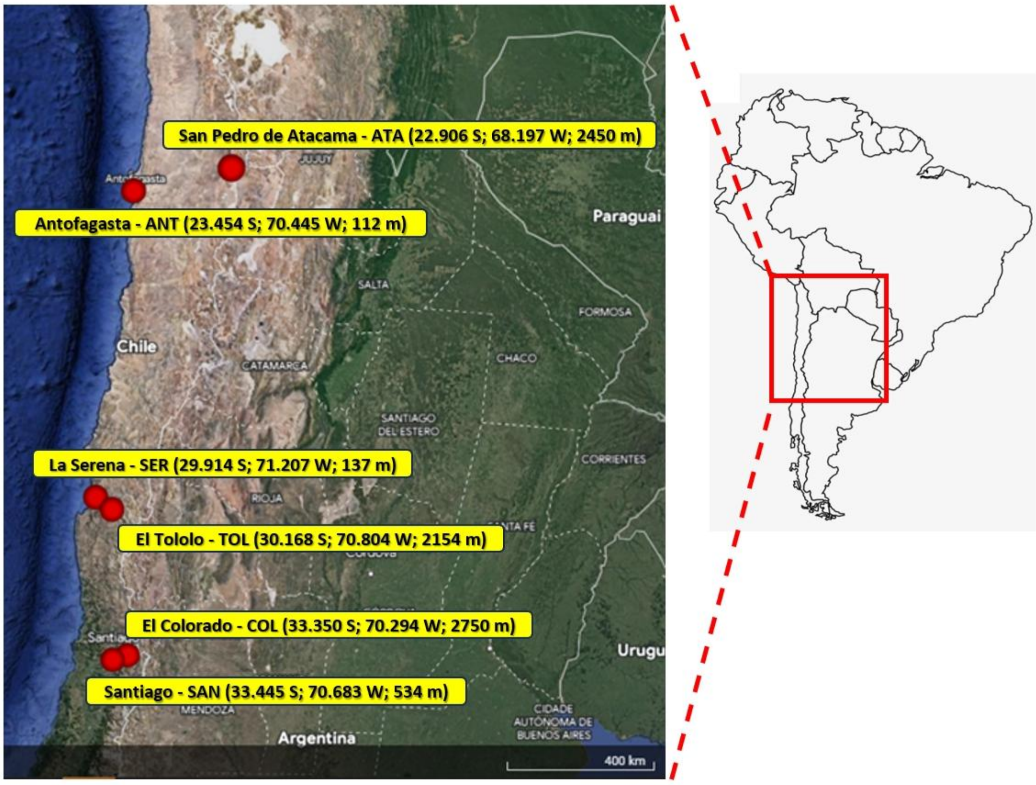

Figure 1. Sites of measurements

Antofagasta is a medium-sized (~390,000 inhabitants) coastal city near the Atacama desert in the North of Chile. It has a highly reflective surface due to the combination of urban cement and desert sand. The climate is desert, one of the regions with the lowest precipitation worldwide, with records of less than 5 mm per decade. Cloud cover is abundant and highly influenced by the low stratus-type cloudiness that develops over the Pacific Ocean due to the solid atmospheric stability of the Eastern South Pacific Subtropical Anticyclone. Thermal amplitude is low throughout the year, with mean annual temperatures around 17°C. The Chilean highlands are part of a considerable extension of the Atacama Desert, characterized by unique characteristics such as very low humidity, high visibility, and high altitudes. For this reason, this area is an ideal natural laboratory to study the increases in UV solar irradiance with height.

On the other hand, San Pedro de Atacama is a small settlement (~3,800 inhabitants) located in the Andes Mountains, far from the oceanic influence. Significant convective rainfall occurs in summer, and is associated with the South American Monsoon. These rains are produced by rising humid air masses from the eastern slopes of the mountain range from the Amazon and Atlantic Ocean. As one moves southward, temperatures decrease, and relative humidity is generally very low throughout the year.

La Serena is also on the coast but further south. Unlike Antofagasta, La Serena shows significant rainfalls during the winter due to the arrival of cold fronts, although the accumulated amounts are relatively low, below 90 mm per year. Towards the interior of the continent, about 50 km southeast of La Serena, on the Tololo hill, the El Tololo measuring station is located. This site shows clear skies, low relative humidity, and significant thermal amplitude predominance. Due to these characteristics and great atmospheric clarity, an important astronomical observatory of the same name has been established there.

Santiago is further south, in the central zone of Chile. The Chilean capital is characterized by a warm-temperate climate with large thermal amplitude during the year, winter rains of mostly frontal origin, and a prolonged dry season between 7 and 8 months, including the summer months. Its average annual temperature is around 15°C. East of Santiago, in the Andes Mountains, is located the El Colorado station, which, unlike Santiago, has higher accumulated rainfall due to the topographic effect (DMC, 2023).

UVR measurements

Erythemal UVR irradiances were measured using YES pyranometers model UVB-1 (YES, 2004). These instruments have a colored glass filter and a highly stable UV-sensitive fluorescent phosphor that converts UVR into visible photons. The instruments were calibrated according to WMO criteria in agreement with the Dirección Meteorológica de Chile (DMC) (WMO, 1995).

Erythemal UVR Irradiances refer to the measurement of UVR weighted by its ability to cause erythema (skin redness or sunburn) in human skin. This concept is crucial in assessing the potential harmful effects of UVR on human health. Erythemal UVR is significant because it is closely associated with harmful effects on human skin, including DNA damage, premature aging, and an increased risk of skin cancer (Farr & Diffey, 1985). As the introduction describes, UVI is the dimensionless representation of erythemal irradiance.

Measurements were collected from 2017 to 2019 when all instruments were calibrated and functional. Data was recorded every second, and the average for every 10 minutes was stored. The following sections describe the analysis of this data.

UVR calculations

Auxiliary UVI calculations were meticulously performed using the Tropospheric Ultraviolet and Visible (TUV) radiation model (Madronick and Flocke, 1997). The TUV model was configured for pristine clear-sky input conditions, cloudless and background aerosols, serving as a reliable reference point for comparison to observations in the absence of relevant local cloud data. We modeled atmospheric scattering and absorption with a multilayer 4-stream discrete ordinates radiative transfer solver, ensuring the utmost precision.

Ozone is the main UVR absorber in the atmosphere. Daily total ozone contents (TOC) were obtained from the Ozone Mapping Instrument (OMI) database (https://aura.gsfc.nasa.gov/omi.html). Figure 2 shows the time series (a) and boxplots (b) of TOC observed between 2017 and 2019 in the study locations. TOC varies seasonally, with maximum values in the austral spring. As expected, locations closer to the equator have lower TOC values than those at higher latitudes. However, ozone is mainly produced in tropical regions, and transport mechanisms in the stratospheric drive the molecules of this gas poleward (Shepherd, 2008; Qu et al., 2023).

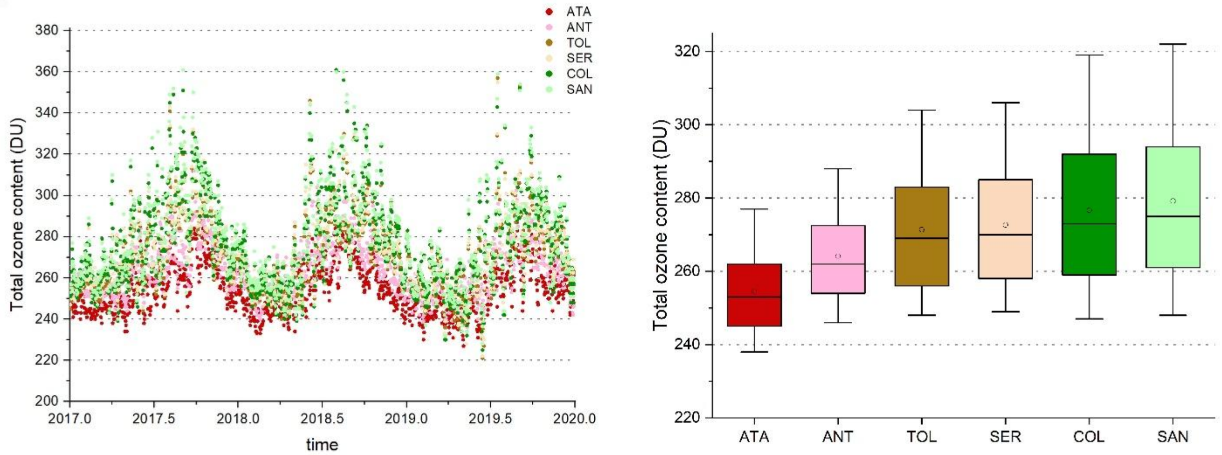

Figure 2. a) Daily variation, and b) boxplots of the TOC between 2017-2019 in San Pedro de Atacama (ATA), Antofagasta (ANT), El Tololo (TOL), La Serena (SER), El Colorado (COL), and Santiago (SAN). Cities are presented from lowest to highest latitude, from left to right. Cities of similar colors are close to each other, with darker colors indicating higher altitudes. In the boxplots, the lower and upper boundaries indicate the 25th and 75th percentiles, respectively. The horizontal line and the circle within the box marks are the median and mean, respectively. Whiskers above and below the box indicate the 5th and 95th percentiles, respectively.

Data analysis

Confidence intervals for UVI ratios at each pair of high (UVI_h) and low (UVI_l) altitude locations were calculated as follows (Bonnet & Price, 2020):

$$\bar{x} - E < \mu < \bar{x} + E \qquad (1)$$

Where:

$x = \frac{UVI_h}{UVI_l}$ and $E = t_{\alpha/2}\frac{s}{\sqrt{n}}$

$t_{\alpha/2}$ has n – 1 degrees of freedom, s is the $\frac{UVI_H}{UVI_L}$ standard deviation and n is the number of UVI measurements.

We considered the following city pairs, ANT/ANT, TOL/SER, and COL/SAN, according to their geographic proximity, for the comparative analysis.

We also calculated the altitude effect (AE) – Equation 2 – as proposed by Schmuki and Philipona (1999); for the AE calculation, only the intensity of UVI and the altitude (z in [m]) at high (h) and low (l) levels, of the specific sites are needed.

$$AE\ (\%) = 100 * \left(\frac{UVI_h - UVI_l}{UVI_h}\right)\left(\frac{1000}{z_h - z_l}\right) \quad (2)$$

Results

Figure 3a shows the boxplots of the daily maximum UVI measurements performed between 2017 and 2019 in the six study sites. On the side, figure 3b shows the numerical simulations for the UVI calculation under clear sky conditions and constant aerosol content. Similar colors represent geographically close locations: Red/Pink - ANT/ANT, Brown/Beige - TOL/SER and Dark Green/Light Green - COL/SAN. Darker colors represent high-altitude sites.

In all locations except SAN, more than half of the UVI measurements exceed the high-risk scale. The average and median UVI values are in the high-risk range for almost all locations. The ATA region stands out for extreme UVI values (> 11) recorded in about 60% of the measurements. Significant UVI values in this high-risk range are also observed in other locations, particularly high-altitude areas. A few recent studies have further explored the relationship between altitude and UVR. For instance, research conducted in the Atacama Desert, characterized by high altitude and prevalent cloudless conditions, has identified this region as having some of Earth's highest surface UV levels (Cordero et al., 2013).

Figure 4 highlights the statistical distribution of the ratio between calculated (TUV) and measured UVI. The ratio UV_{TUV}/UV_{meas} is consistently greater than 1 because TUV calculations are based on clear sky conditions, without clouds, and constant aerosol concentrations and ground reflection. The highest UVI measurements in this study occurred on clear-sky days. However, the presence of clouds, particularly cirrus, increased aerosol concentrations, or decreased ground reflectance can diminish the amount of UVI at the surface. Further investigation is crucial to determine the impact of these variables in this region, especially in assessing the effects of climate change.

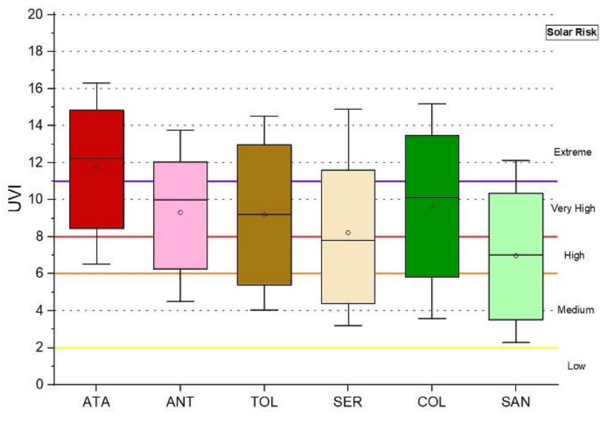

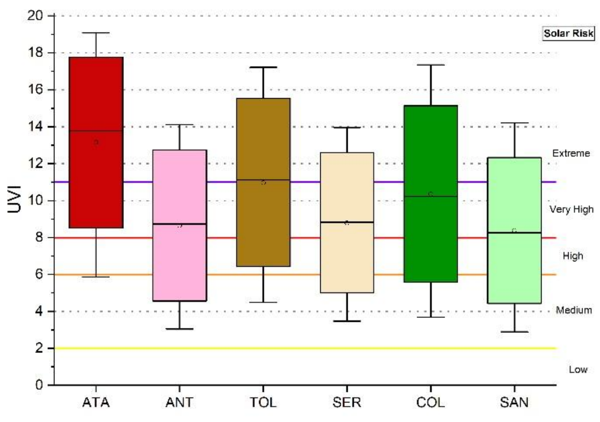

Figure 3. Boxplots of the daily maximum UVI measurements (**a**) and calculations (**b**) between 2017-2019 in San Pedro de Atacama (ATA), Antofagasta (ANT), El Tololo (TOL), La Serena (SER), El Colorado (COL), and Santiago (SAN). Cities are presented from lowest to highest latitude, from left to right. Cities of similar colors are close to each other, with darker colors indicating higher altitudes. The boxplot's lower and upper boundaries indicate the 25th and 75th percentiles, respectively. The horizontal black line and the circle within the box marks are the median and mean, respectively. Whiskers above and below the box indicate the 5th and 95th percentiles, respectively. The colored horizontal lines in the background indicate the risk scale for UVI (see Table 1).

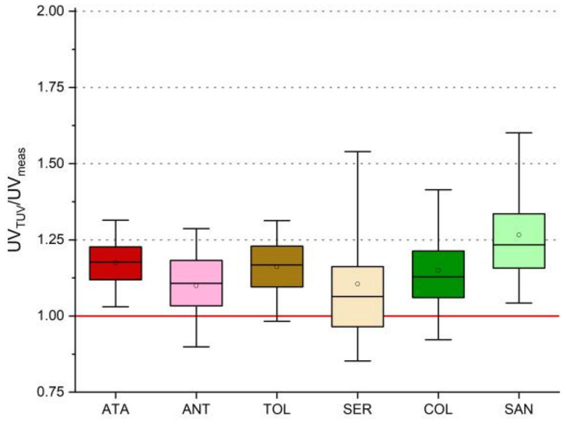

Figure 4. Boxplot of the quotient between calculated (TUV) and measured UVI. In the boxplots, the lower and upper boundaries indicate the 25th and 75th percentiles, respectively. The horizontal line and the circle within the box marks are the median and mean, respectively. Whiskers above and below the box indicate the 5th and 95th percentiles, respectively.

The impact of altitude on the UVI is observed in Figure 5. The altitude differences between ATA and ANT, TOL and SER, and COL and SAN equal 2338 m, 2017 m, and 2216 m, respectively (see Figure 1). The confidence intervals for the mean ratios of UVI measured in the three pairs of cities were as follows: ATA/ANT - [1.28; 1.30]; TOL/SER = [1.14;1.17]; COL/SAN - [1.36; 1.39] (p-value < 0.001 for all). These values are comparable to those obtained for altitudes between 0 and 3000 m with and without snow-covered surfaces (Ambach, 1993).

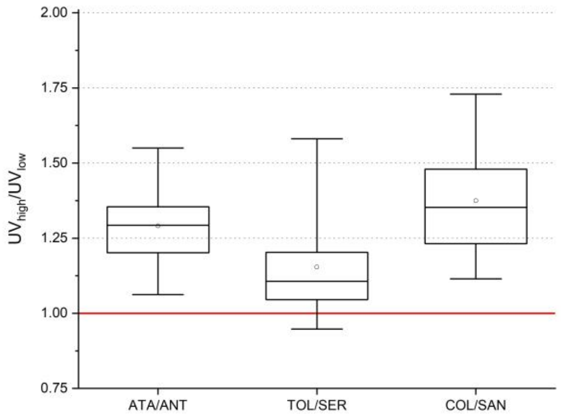

Figure 5. Boxplot of the relative difference between UVI at altitude and at sea level observed between nearby cities. In the boxplots, the lower and upper boundaries indicate the 25th and 75th percentiles, respectively. The horizontal line and the circle within the box marks are the median and mean, respectively. Whiskers above and below the box indicate the 5th and 95th percentiles, respectively.

Figure 6 shows the AE bloxplots.The 95% confidence intervals for ATA/ANT are [9.0; 9.5], for TOL/SER are [5.3; 6.1], and for COL/SAN are [11.2; 11.9] (p-value < 0.001 for all). These confidence intervals can be compared to those obtained by Schmucki and Philipona (2002) for the Swiss Alps, with altitudes ranging from 1600m to 3600m. The study for the Swiss Alps involved comparing three measuring stations, with average results ranging from 4.4 to 13.2, excluding questionable values as identified by the authors.

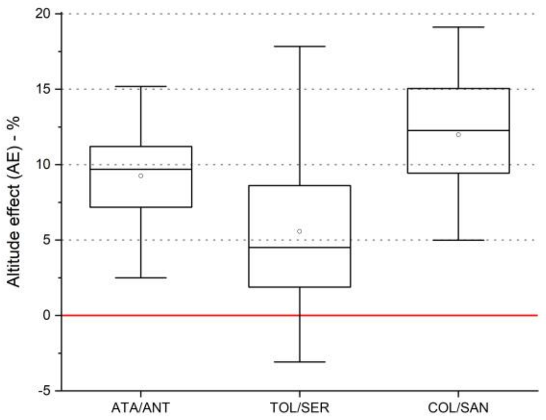

Figure 6. Boxplot of the relative difference between AE at altitude and at sea level observed between nearby cities. In the boxplots, the lower and upper boundaries indicate the 25th and 75th percentiles, respectively. The horizontal line and the circle within the box marks are the median and mean, respectively. Whiskers above and below the box indicate the 5th and 95th percentiles, respectively.

Final Remarks

Over three years, simultaneous measurements of the UVI were conducted at six Chile sites, three at sea level and three at mountain tops. The average altitude effect on the measured UVI ranged from 5.7% to 11.6% per 1000 meters, corresponding to a mean high-low altitude ratio between 1.15 and 1.37. Consistent with previous studies, the AE is not constant and is influenced by factors such as solar position, surface reflectance, and air turbidity. Comparisons between UVI measurements and theoretical simulations using the Tropospheric Ultraviolet and Visible (TUV) radiative transfer model for clear-sky conditions revealed that the model's UVI results were 15% to 27% higher than the observed data.

Additionally, variations in the AE on the UVI were consistent, with average fluctuations between

9% and 11%. The scientific literature presents limited studies on the effects of altitude on UVR, underscoring the need for further research to determine the impact of surface cover (such as snow, sand, or asphalt) and air pollution. This gap opens avenues for future investigations.

The results emphasize the importance of reinforcing photoprotection measures when visiting high altitudes. The high-altitude locations studied are often used for sports or leisure activities. However, due to a lack of awareness or adherence to daily habits, appropriate photoprotection measures for exposure in these locations are sometimes overlooked. This highlights the need for public awareness and individual responsibility in ensuring adequate photoprotection.

Acknowledgments

MPC thanks Fapemig (#APQ-00768-18) and CNPq (#309294/2023-1). DL acknowledges partial financial support from Centers of Excellence with BASAL/ANID financing, AFB220001, CEDENNA. LMP acknowledges financial support from ANID through Convocatoria Nacional Subvención a Instalación en la Academia Convocatoria, año 2021, Grant SA77210040.

References

Alonso, F., Garmendia, M., & Bogado, M. (2010). Increased skin cancer mortality in Chile Beyond the Effect of Ageing: Temporal Analysis 1990 to 2005. *Acta Dermato Venereologica*, *90*(2), 141–146. https://doi.org/10.2340/00015555-0787

Ambach, W., Blumthaler, M., & Schöpf, T. (1993). Increase of biologically effective ultraviolet radiation with altitude. *Journal of Wilderness Medicine*, *4*(2), 189–197. https://doi.org/10.1580/0953-9859-4.2.189

Arias, L. A., Berli, F., Fontana, A., Bottini, R., & Piccoli, P. (2022). Climate change Effects on grapevine Physiology and Biochemistry: Benefits and Challenges of High Altitude as an adaptation Strategy. *Frontiers in Plant Science*, *13*. https://doi.org/10.3389/fpls.2022.835425

Barnes, P. W., Williamson, C. E., Lucas, R. M., Robinson, S. A., Madronich, S., Paul, N. D., Bornman, J. F., Bais, A. F., Sulzberger, B., Wilson, S. R., Andrady, A. L., McKenzie, R. L., Neale, P. J., Austin, A. T., Bernhard, G. H., Solomon, K. R., Neale, R. E., Young, P. J., Norval, M., . . . Zepp, R. G. (2019). Ozone depletion, ultraviolet radiation, climate change and prospects for a sustainable future. *Nature Sustainability*, *2*(7), 569–579. https://doi.org/10.1038/s41893-019-0314-2

Bloch, L. D., Valente, N. Y. S., Escudeiro, C. C., Sarruf, F. D., & Velasco, M. V. R. (2020). Chemical and physical damage affect the perceptions of hair attributes: A quantitative sensory assessment by a trained panel. *Journal of Sensory Studies*, *36*(1). https://doi.org/10.1111/joss.12621

Bonett, D. G., & Price, R. M. (2020). Confidence intervals for ratios of means and medians. *Journal of Educational and Behavioral Statistics*, *45*(6), 750–770. https://doi.org/10.3102/1076998620934125

Cabrera, S., Bozzo, S., & Fuenzalida, H. (1995). Variations in UV radiation in Chile. *Journal of Photochemistry and Photobiology B Biology*, *28*(2), 137–142. https://doi.org/10.1016/1011-1344(94)07103-u

Cedirian, S., Prudkin, L., Piraccini, B. M., Santamaria, J., Piquero-Casals, J., & Saceda-Corralo, D. (2024). The exposome impact on hair health: etiology, pathogenesis and clinical features – Part I. *Anais Brasileiros De Dermatologia*. https://doi.org/10.1016/j.abd.2024.07.003

Cordero, R. R., Seckmeyer, G., Damiani, A., Riechelmann, S., Rayas, J., Labbe, F., & Laroze, D. (2013). The world's highest levels of surface UV. *Photochemical & Photobiological Sciences*, *13*(1), 70–81. https://doi.org/10.1039/c3pp50221j

Corrêa, M. P., Yamamoto, A. L. C., Moraes, G. R., Godin-Beekmann, S., & Mahé, E. (2019). Changes in the total ozone content over the period 2006 to 2100 and the effects on the erythemal and vitamin D effective UV doses for South America and Antarctica. *Photochemical & Photobiological Sciences*, *18*(12), 2931–2941. https://doi.org/10.1039/c9pp00276f

Corrêa, M.P. (2015). Solar ultraviolet radiation: properties, characteristics and amounts observed in Brazil and South America. *Anais Brasileiros De Dermatologia*, *90*(3), 297–313. https://doi.org/10.1590/abd1806-4841.20154089

Diffey, B. L. (1991). Solar ultraviolet radiation effects on biological systems. *Physics in Medicine and Biology*, *36*(3), 299–328. https://doi.org/10.1088/0031-9155/36/3/001

Ding, P., Zhang, Y., & He, Y. (2024). Risk factors for pterygium: Latest research progress on major pathogenesis. *Experimental Eye Research*, *243*, 109900. https://doi.org/10.1016/j.exer.2024.109900

DMC – *Servicios climáticos de Chile*. (2024). https://climatologia.meteochile.gob.cl/application/publicaciones/documentoPdf/anuario/anuario-2023.pdf

Farr, P., & Diffey, B. (1985). The erythemal response of human skin to ultraviolet radiation. *British Journal of Dermatology*, *113*(1), 65–76. https://doi.org/10.1111/j.1365-2133.1985.tb02045.x

Fitzpatrick, T. B. (1988). The validity and practicality of sun-reactive skin types I through VI. *Archives of Dermatology*, *124*(6), 869–871. https://doi.org/10.1001/archderm.124.6.869

Frazão, L. F. N., Cruvinel, L. M., Da Silva, A. L. P., Silva, G. H., Juntolli, A. C. V., De Azevedo, A. F., Naser, M. S. R. H., Piveta, J. T., Oliveira, M. E. G., Mota, M. C. W., Santos, L. P., Ferreira, L. F., Cabral, M. C., & Zanoni, R. D. (2024). Resultâncias fisiobiológicas da radiação ultravioleta e suas funções na carcinogênese de pele. *Brazilian Journal of Implantology and Health Sciences*, *6*(1), 833–842. https://doi.org/10.36557/2674-8169.2024v6n1p833-842

Gerstein, W. S. C.-., & Samaniego, G. T.-. (2021). High altitude and cancer: An old controversy. *Respiratory Physiology & Neurobiology*, *289*, 103655. https://doi.org/10.1016/j.resp.2021.103655

Hart, P. H., & Norval, M. (2021). More than effects in skin: ultraviolet Radiation-Induced changes in immune cells in human blood. *Frontiers in Immunology*, *12*. https://doi.org/10.3389/fimmu.2021.694086

Hatsusaka, N., Yamamoto, N., Miyashita, H., Shibuya, E., Mita, N., Yamazaki, M., Shibata, T., Ishida, H., Ukai, Y., Kubo, E., Cheng, H., & Sasaki, H. (2021). Association among pterygium, cataracts, and cumulative ocular ultraviolet exposure: A cross-sectional study in Han people in China and Taiwan. *PLoS ONE*, *16*(6), e0253093. https://doi.org/10.1371/journal.pone.0253093

ISO/CIE 1999, ISO 17166:1999(E)/CIE S 007/E-1998: Joint ISO/CIE Standard: Erythema Reference Action Spectrum and Standard Erythema Dose, Geneva: ISO/Vienna: CIE.

Kliniec, K., Tota, M., Zalesińska, A., Łyko, M., & Jankowska-Konsur, A. (2023). Skin Cancer Risk, Sun-Protection Knowledge and Behavior in Athletes—A Narrative Review. *Cancers*, *15*(13), 3281. https://doi.org/10.3390/cancers15133281

Liang, X., Zhang, C., Shen, L., Ding, L., & Guo, H. (2024). Role of non-coding RNAs in UV-induced radiation effects (Review). *Experimental and Therapeutic Medicine*, *27*(6). https://doi.org/10.3892/etm.2024.12550

Madronich, S., Flocke, S. (1997). Theoretical Estimation of Biologically Effective UV Radiation at the Earth's Surface. In: Zerefos, C.S., Bais, A.F. (eds) Solar Ultraviolet Radiation. NATO ASI Series, vol 52. Springer, Berlin, Heidelberg. https://doi.org/10.1007/978-3-662-03375-3_3

Marilyn, A. E., Marcelo, M. S., Ivar, A. P., James, A. E., Pablo, A. M., Ximena, H. L., & Karen, A. T. (2024). Climate change, ultraviolet radiation and sensitive ocular diseases in high altitude population. In *Climate change management* (pp. 95–127). https://doi.org/10.1007/978-3-031-72740-5_6

Parisi, A., Igoe, D., Downs, N., Turner, J., Amar, A., & Jebar, M. A. (2021). Satellite monitoring of environmental Solar Ultraviolet A (UVA) exposure and irradiance: A review of OMI and GOME-2. *Remote Sensing*, *13*(4), 752. https://doi.org/10.3390/rs13040752

Patra, V., Bordag, N., Clement, Y., Köfeler, H., Nicolas, J., Vocanson, M., Ayciriex, S., & Wolf, P. (2023). Ultraviolet exposure regulates skin metabolome based on the microbiome. *Scientific Reports*, *13*(1). https://doi.org/10.1038/s41598-023-34073-3

Qu, K., Wang, X., Cai, X., Yan, Y., Jin, X., Vrekoussis, M., Kanakidou, M., Brasseur, G. P., Shen, J., Xiao, T., Zeng, L., & Zhang, Y. (2023). Rethinking the role of transport and photochemistry in regional ozone pollution: insights from ozone concentration and mass budgets. *Atmospheric Chemistry and Physics*, *23*(13), 7653–7671. https://doi.org/10.5194/acp-23-7653-2023

Reshi, A. R., Pichuka, S., & Tripathi, A. (2024). Applications of Sentinel-5P TROPOMI Satellite Sensor: A review. *IEEE Sensors Journal*, *24*(13), 20312–20321. https://doi.org/10.1109/jsen.2024.3355714

Schmalwieser, A. W., Casale, G. R., Colosimo, A., Schmalwieser, S. S., & Siani, A. M. (2021). Review on occupational personal solar UV exposure measurements. *Atmosphere*, *12*(2), 142. https://doi.org/10.3390/atmos12020142

Schmucki, D. A. (2002). Ultraviolet radiation in the Alps: the altitude effect. *Optical Engineering*, *41*(12), 3090. https://doi.org/10.1117/1.1516820

Shepherd, T. G. (2008). Dynamics, stratospheric ozone, and climate change. *ATMOSPHERE-OCEAN*, *46*(1), 117–138. https://doi.org/10.3137/ao.460106

Silva, A. A., Yamamoto, A. L. C., & Corrêa, M. P. (2018). Daily maximum erythemal dose rates in the tropics. *Photochemistry and Photobiology*, *95*(3), 886–894. https://doi.org/10.1111/php.13054

Vuilleumier, L., Harris, T., Nenes, A., Backes, C., & Vernez, D. (2020). Developing a UV climatology for public health purposes using satellite data. *Environment International*, *146*, 106177. https://doi.org/10.1016/j.envint.2020.106177

WHO, World Health Organization (2002). Global Solar UV Index: A Practical Guide, 2002, WHO/SDE/OEH/02.2, 28 pp, Geneva, Switzerland. https://www.who.int/publications/i/item/9241590076

WHO, World Meteorological Organization (2022). Executive Summary. Scientific Assessment of Ozone Depletion: 2022, GAW Report No. 278, 509 pp., Geneva, Switzerland. https://ozone.unep.org/sites/default/files/2023-02/Scientific-Assessment-of-Ozone-Depletion-2022.pdf

WHO, World Meteorological Organization (1995). UV Monitoring and Assessment Program Panel Report of the WMO Meeting of Experts on UV-B Measurements, Data Quality and Standardization of UV Indices, GAW Report No. 95, Geneva, Switzerland. https://library.wmo.int/idurl/4/41287

Yamamoto, A. L. C., De Paula Corrêa, M., Torres, R. R., Martins, F. B., & Godin-Beekmann, S. (2024). Projected changes in ultraviolet index and UV doses over the twenty-first century: impacts of ozone and aerosols from CMIP6. *Photochemical & Photobiological Sciences*, *23*(7), 1279–1294. https://doi.org/10.1007/s43630-024-00594-7

Yamamoto, A. L. C., De Paula Corrêa, M., Torres, R. R., Martins, F. B., & Godin-Beekmann, S. (2024a). Total ozone content, total cloud cover, and aerosol optical depth in CMIP6: simulations performance and projected changes. *Theoretical and Applied Climatology*, *155*(3), 2453-2471. https://doi.org/10.1007/s00704-023-04821-6

YES - Yankee Environmmental System (2004). Bulletin UVB-3S. Ultraviolet pyranometer model UVB-1/UVA-1. https://www.yesinc.com/resource/products/solarradiation/uvb-1ds.pdf

Zemelman, V., Roa, J., Díaz, C., Araya, I., Zamalloa, G., Faúndez, E. Aumento de la incidencia de cáncer cutáneo en hospitales públicos de la región metropolitana (1992-1998). *Revista Chilena de Dermatologia, 17(3)*, 180-185.

Zerefos, C., Fountoulakis, I., Eleftheratos, K., & Kazantzidis, A. (2023). Long-term variability of human health-related solar ultraviolet-B radiation doses from the 1980s to the end of the 21st century. *Physiological Reviews*, *103*(3), 1789–1826. https://doi.org/10.1152/physrev.00031.2022